(a)

(b)

Fig. 5. Current transfer and input current-to-voltage characteristics.

on linear approximation of the $I–V$ characteristics, and the class-AB current mirror allows to do the linear approximation for relatively large signal current swing. This leads to the reduction of the harmonic distortion due to the nonlinearity of the $I–V$ characteristics.

IV. CONCLUSIONS

This brief describes the property of the high-precision class-AB current mirror. The complementary current transfer nature allows us to reduce the bias current compared to the signal current, and this property leads to the reduction of the mismatch sensitivity to the current offset error. The basic idea of this class-AB current-mirror can be also applied to switched-current signal processing circuits.

REFERENCES

[1] S. S. Lee, R. H. Zele, D. J. Allstot, and G. Liang, "CMOS continuous-time current-mode filters for high-frequency applications," *IEEE J. Solid-State Circuits*, vol. 27, pp. 323–329, 1993.

[2] J. B. Hughes, N. C. Bird, and J. C. Macbeth, "Switched currents–A new technique for sampled-data signal processing," in *Proc. IEEE Int. Symp. Circuits Syst.*, 1989, pp. 1584–1587.

[3] J. R. Angulo, "Wide range gain programmable class AB linear current mirrors for low supply voltage operation," *IEEE Trans. Circuits Syst. II*, vol. 41, pp. 631–634, Sept. 1994.

[4] Z. Wang, "Wideband class AB (push pull) current amplifier in CMOS technology," *Electron. Lett.*, vol. 26, pp. 543–545, Apr. 1990.

[5] K. R. Lakshmikumar, R. T. Hadaway, and M. A. Copeland, "Characterization and modeling of mismatch in MOS transistors for precision analog design," *IEEE J. Solid-State Circuits*, vol. SC-21, pp. 1057–1066, 1986.

[6] M. J. M. Pelgrom, A. C. J. Duinmaijer, and A. P. G. Welbers, "Matching properties of MOS transistors," *IEEE J. Solid-State Circuits*, vol 24, pp. 1433–1440, 1989.

Suppressing Chaos with Hysteresis in a Higher Order Neural Network

Lipo Wang

Artificial neural networks (ANN's) attempt to mimic various features of a most powerful computational system—the human brain. Since ANN's consist of a large number of parallel array of simple processing elments (neurons), they are naturally suited for today's fast-developing VLSI technology. For instance, Linares-Barranco *et al.* [1] designed a programmable analog neural oscillator with hysteresis appropriate for monolithic integrated circuits. Dynamic systems have many applications; however, stability is often desired. We show analytically that hysteresis at the single neuron level can provide a simple means to preserve stability in an ANN even when the nature of the system is chaotic.

Wang and Ross [2] studied static retrieval performance of a network of binary hysteretic neurons in the presence of random noise. They showed that neuronal hysteresis, which results in a tendency for each neuron to remain in its current state, helps the neurons to resist random signals and avoid random response, thereby improving the overall retrieval ability of the network. Through numerical simulations to solve an optimization problem, Takefuji and Lee [3] used binary hysteretic neurons to accelerate the convergence to the global minimum by suppressing oscillatory behaviors encountered during the convergence process. However, these oscillatory behaviors should be considered numerical artifacts, since the dynamics in neural networks used for these optimization problems are nonoscillatory and the convergence process represents a descent on a Lyapnov energy surface.

In this brief we consider N binary hysteretic neurons with the following updating rule (Fig. 1) (see (1) at the top of the next page) where $S_i(t)$ represents the state of neuron i at time t and α is the half-width of the bistable region. The total input for neuron i is

$$h_i(t) = \gamma_1 \sum_{j=1}^{N} T_{ij} S_j(t) + \gamma_2 \sum_{j,k=1}^{N} T_{ijk} S_j(t) S_k(t) + \eta_i \quad (2)$$

where

$$T_{ij} = C_{ij} \sum_{\mu=1}^{p} S_i^{\mu} S_j^{\mu} \quad \text{and} \quad T_{ijk} = C_{ijk} \sum_{\mu=1}^{p} S_i^{\mu} S_j^{\mu} S_k^{\mu} \quad (3)$$

are the modified first- and second-order Hebbian synaptic efficacies, $\vec{S}^{\mu}$ is the μth stored pattern, and p is the number of patterns stored. The coefficients γ_1 and γ_2 measure the relative strengths of first- and second-order interactions. We have introduced synaptic disruptions in the efficacies T_{ij} and T_{ijk} by choosing random variables C_{ij} and C_{ijk} as follows: C_{ij} is 1 with a probability (C/N), C_{ijk} is 1 with a probability $(2C/N^2)$, C_{ij} and C_{ijk} are zero otherwise. We also include in (2) a background Gaussian noise η_i with a standard deviation σ_o in order to take into account the presence of signal transmission noise.

In the absence of neuronal hysteresis ($\alpha = 0$), the above higher-order system was discussed by Wang, Pichler, and Ross [4]. The

$$S_i(t+1) = \begin{cases} +1 \text{ if } S_i(t) = +1 \text{ and } h_i(t) > -\alpha; \text{ or } S_i(t) = -1 \text{ and } h_i(t) > \alpha \\ -1 \text{ if } S_i(t) = +1 \text{ and } h_i(t) \leq -\alpha; \text{ or } S_i(t) = -1 \text{ and } h_i(t) \leq \alpha \end{cases} \qquad (1)$$
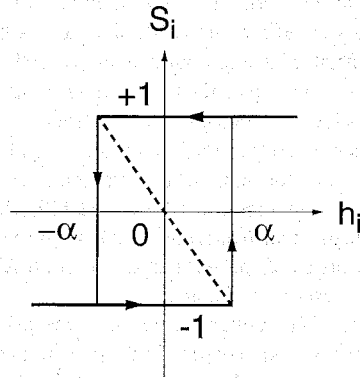

Fig. 1.   Input–output response functions for a binary artificial neuron with hysteresis.

network dynamics in the presence of neuronal hysteresis can be obtained analytically in a similar fashion

$$
\begin{aligned}
m(t+1) &= \left[\frac{1+m(t)}{2}\right] \mathrm{erf}\left\{\frac{\gamma_1 m(t) + \gamma_2 [m(t)]^2 + \alpha'}{\sqrt{2}\sigma}\right\} \\
&+ \left[\frac{1-m(t)}{2}\right] \mathrm{erf}\left\{\frac{\gamma_1 m(t) + \gamma_2 [m(t)]^2 - \alpha'}{\sqrt{2}\sigma}\right\}
\end{aligned} \qquad (4)
$$

where $\alpha' = \alpha/C$, $m(t) = \langle \vec{S}(t) \cdot \vec{S}^1 \rangle / N$ is a statistical average of the overlap between the state of the network and the stored pattern to which the network is initially close. $\sigma \equiv \sqrt{(\gamma_1^2 + \gamma_2^2)(p-1)/C + (\sigma_o/C)^2}$ is a rescaled noise level that represents the combined effects of the random synaptic disruption, interference between stored patterns, and additional background noise.

Fig. 2 shows iterative solutions of the dynamic equation (4) for various widths of the bistable region in the neuronal hysteresis in the case where $\gamma_1 = 1$ and $\gamma_2 = -1$. Fig. 2(a) shows the case without neuronal hysteresis, where abundant oscillatory and chaotic activities are evident. When a small amount of neuronal hysteresis is introduced, chaos is first suppressed [Fig. 2(b)]. As the hysteretic width increases, chaos disappears and periodic oscillations also become suppressed [Fig. 2(c)]. The system becomes completely stable for $\alpha' \geq 0.1$.
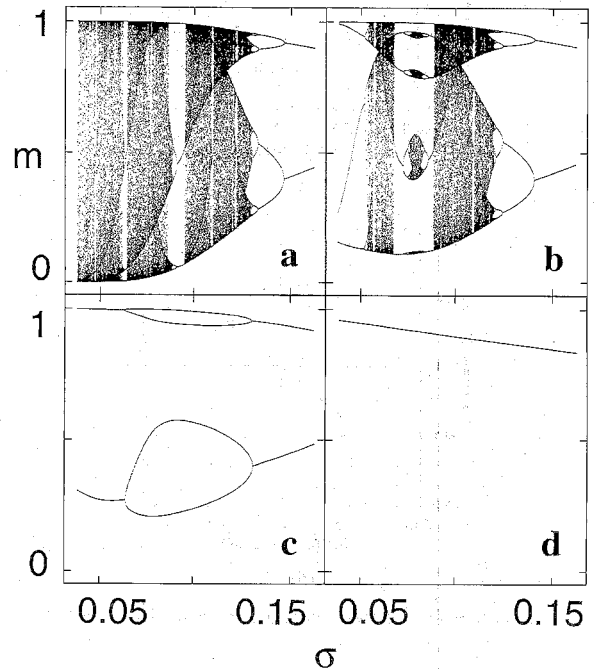

Fig. 2.   Solutions (fixed points) of m given by dynamic equation (4), the overlap between the state of the network and the initial attracting memory pattern, as a function of the rescaled noise level σ (a) in the absence of hysteresis, i.e., $\alpha' = 0$. (b) $\alpha' = 0.01$, incomplete bifurcation and suppressed chaotic region. (c) $\alpha' = 0.02$ reduction of chaos to oscillations with periods no greater than 4. (d) $\alpha' = 0.1$ disappearances of both chaos and periodic oscillations.

REFERENCES

[1] B. Linares-Barranco, E. Sanchez-Sinencio, A. Rodrigues-Vazquez, and J. L. Huertas, "A programmable neural oscillator cell," *IEEE Trans. Circuits Syst.*, vol. 36, pp. 756–761, 1989.

[2] L. Wang and J. Ross, "Synchronous neural networks of nonlinear threshold elements with hysteresis," in *Proc. Nat. Acad. Sci.*, vol. 87, Feb. 1990, pp. 988–992.

[3] Y. Takefuji and K. C. Lee, "An artificial hysteresis binary neuron: A model suppressing the oscillatory behaviors of neural dynamics," *Biol. Cybern.*, vol. 64, pp. 353–356, 1991.

[4] L. Wang, E. E. Pichler, and J. Ross, "Oscillations and chaos in neural networks: An exactly solvable model," in *Proc. Nat. Acad. Sci.*, Dec. 1990, vol. 87, pp. 9467–9471.